



Modeling of thundercloud screening charges: Implications for blue and gigantic jets

Jeremy A. Rioussset,¹ Victor P. Pasko,¹ Paul R. Krehbiel,² William Rison,³
and Mark A. Stanley⁴

Received 23 March 2009; revised 17 August 2009; accepted 28 August 2009; published 22 January 2010.

[1] A two-dimensional axisymmetric model of charge relaxation in the conducting atmosphere is used in conjunction with a probabilistic lightning model to demonstrate how realistic cloud electrodynamics lead to the development of blue and gigantic jets. The model accounts for time-dependent conduction currents and screening charges formed under the influence of the thundercloud charge sources. Particular attention is given to numerical modeling of the screening charges near the cloud boundaries. The modeling results demonstrate the important role of the screening charges in local enhancement of the electric field and/or reduction of net charge in the upper levels of the thundercloud. The charge relaxation model presented in this work confirms the previous results obtained with a simpler model by Krehbiel et al. (2008), specifically that the accumulation of screening charges near the thundercloud top produces a charge configuration leading to the initiation of blue jets, while the effective mixing of these charges with the upper thundercloud charge may lead to the formation of gigantic jets.

Citation: Rioussset, J. A., V. P. Pasko, P. R. Krehbiel, W. Rison, and M. A. Stanley (2010), Modeling of thundercloud screening charges: Implications for blue and gigantic jets, *J. Geophys. Res.*, 115, A00E10, doi:10.1029/2009JA014286.

1. Introduction

[2] Krehbiel et al. [2008] demonstrated how charge imbalances in the thundercloud lead to the development of various types of lightning discharges, including upward directed electrical discharges, so-called blue jets [Wescott et al., 1995; Sentman and Wescott, 1995; Boeck et al., 1995; Wescott et al., 2001] and gigantic jets [Pasko et al., 2002; Su et al., 2003; van der Velde et al., 2007; Chen et al., 2008a, 2008b; Kuo et al., 2009]. The phenomenology of the different types of upward discharges observed to date has been recently reviewed by Mishin and Milikh [2008] and Pasko [2008]. In addition to local and global thundercloud charge, imbalances created by cloud-to-ground or intracloud discharges prior to the initiation of jets, Krehbiel et al. [2008] also emphasized the role of the screening charge forming around the thundercloud boundaries in the development of both kinds of jets. The screening charge is responsible for two effects. First, it reduces the net overall charge content in the upper part of the storm by offsetting and mixing with the upper storm charge, as first suggested by Wilson [1921]. The screening charge results from electrical

conduction currents to the cloud boundary and forms relatively rapidly around the upper boundary because of the significant increase in the atmospheric conductivity with altitude. When strongly mixed with the upper storm charge, the screening charge produces a charge imbalance that enables intracloud discharges to escape upward or outward from the storm as gigantic jets or bolt from the blue discharges. The second effect is that, when not mixed or otherwise removed, the screening charge enhances the electric field immediately below the upper cloud boundary, by virtue of constituting an additional concentrated charge region. This last hypothesis was initially explored with Krehbiel et al.'s [2004] model to demonstrate how the enhanced electric field at the top of the thunderstorm explains the development of blue jets and was further investigated with an improved version of this model in the work of Krehbiel et al. [2008, supplementary information].

[3] The electrodynamic model of the study by Krehbiel et al. [2008] represented the effects of the cloud being embedded in a conductive atmosphere by determining the current density $J_z = \sigma(z_{\text{top}})E_z$ that would occur in the clear air immediately above the cloud top. The current density was calculated from the electric field E_z on the axis of a cylindrical disk model due to the interior storm charges and from the atmospheric electric conductivity $\sigma(z = z_{\text{top}})$, where z is the vertical coordinate representing the altitude. The current density was assumed to be constant over the effective area A of the cloud top charge disk and to thereby cause a total current $I_{\text{SC}} = J_z A$ that would accumulate at the upper cloud boundary as a screening charge. The presence of the screening charge in turn reduced the electric field above the storm top, which in the absence of interior

¹CSSL Laboratory, Department of Electrical Engineering, Pennsylvania State University, University Park, Pennsylvania, USA.

²Department of Physics, New Mexico Institute of Mining and Technology, Socorro, New Mexico, USA.

³Department of Electrical Engineering New Mexico Institute of Mining and Technology, Socorro, New Mexico, USA.

⁴Jemez Springs, New Mexico, USA.

charging causes the exterior field to relax exponentially with time with a time constant ε_0/σ . This constituted a one-dimensional approach for modeling atmospheric charge relaxation that was approximately correct for the parallel plate cylindrical charge model of the study.

[4] In the present work the charge relaxation process is modeled more accurately and in more detail using a fully two-dimensional axisymmetric model that takes into account the increase of atmospheric conductivity $\sigma(z)$ with altitude z in and around the cloud boundaries. In addition to describing the dynamical formation of the screening charge, the model provides a complete picture of the interior and exterior electric field, charges, and potential. The model also introduces self-consistent reassignment of the net charge contents in the cloud charge layers as a result of the occurrence of a sequence of lightning discharges. The relaxation determination employs a macroscopic approach similar to that used by *Pasko et al.* [1997] and does not involve or require explicit treatment of atmospheric ions [e.g., *Helsdon and Farley*, 1987]. Results of the cloud electrodynamic model are used as the basis for three-dimensional simulations of individual lightning discharges [*Riousset et al.*, 2007], as an initial means of self-consistently determining the complete electrical evolution of a storm. The 2-D electrostatic formulation employed in this work does not allow incorporating dynamical cloud processes such as charge advection, storm top divergence, or deformation of charge layers by an updraft, but their potential effects will be discussed in section 4.

[5] The two effects of the charge relaxation process, namely the magnification of electric field and dissipation of the upper storm charge can be illustrated by means of two examples, presented in Figures 1 and 2 (see Animations S1, S2a, and S2b of the auxiliary material).¹ The distributions of electric charges in the examples are purposely exaggerated and simplified in comparison with realistic distributions to accentuate the effects discussed later in this paper in connection with the development of blue and gigantic jets.

[6] Figure 1 illustrates how, when two equal and opposite polarity charges are placed in an infinite conductive medium with conductivity increasing with altitude, the overall system develops an excess of charge of the polarity of the lower charge due to the differences in relaxation time scales of charges at different altitudes [*Wilson*, 1921]. To simulate open boundary conditions we adopt a formulation similar to that described by *Liu and Pasko* [2006]. For the case when conductivity increases with altitude, the time scale of the charge dissipation $\tau_\sigma(z)$ is given by $\tau_\sigma(z) = \varepsilon_0/\sigma(z) = (\varepsilon_0/\sigma_0) e^{-z/h}$, where ε_0 , $\sigma(z)$, σ_0 , and h are the free space permittivity, the conductivity of the medium as a function of the altitude z , the conductivity at sea level, and the conductivity's characteristic height, respectively [e.g., *Brown et al.*, 1971; *Pasko et al.*, 1997, Appendix B]. Since σ increases with z , the upper positive charge (+) in Figure 1 dissipates faster than the lower negative charge (-), yielding an excess of negative charge in the system (see Animation S1). In the example shown, $\tau_\sigma(25.6 \text{ km}) = \tau_\sigma^+ = 2.45 \text{ s}$ for the upper positive charge and $\tau_\sigma(12.8 \text{ km}) = \tau_\sigma^- = 20.8 \text{ s}$ for the lower negative charge. Figure 1b shows a cross-sectional view of

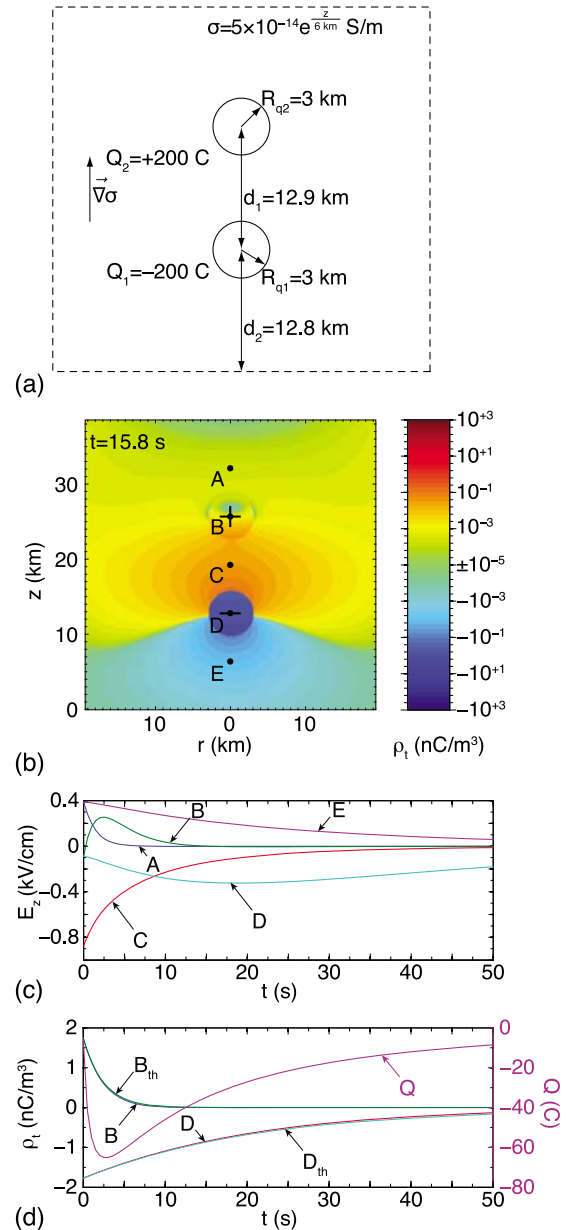


Figure 1. Charge dissipation in a conductive medium as a function of the altitude. (a) Geometry of the illustrative example. (b) Cross-sectional view of the charge density distribution at $t \sim 15.8 \text{ s}$. The positive charge (+) has almost disappeared, while the negative charge (-) has only slightly dissipated. Letters A–E indicate the loci of observation of the evolution of the (c) electric field and (d) charge density, respectively. In Figure 1d, B_{th} and D_{th} indicate the analytically calculated approximations of the evolutions of the charge densities at points B and D. The total charge Q in the simulation domain is represented using a solid purple line with corresponding scale shown on the right vertical axis. (See Animation S1 for the animated version Figure 1b.)

the charge density after 15.8 s, i.e., after $\sim 6.5\tau_\sigma^+$ and $\sim .75\tau_\sigma^-$. By this time the positive charge has almost completely dissipated, whereas the negative charge is mostly intact. The system develops an excess of negative

¹Auxiliary materials are available in the HTML. doi:10.1029/2009JA014286.

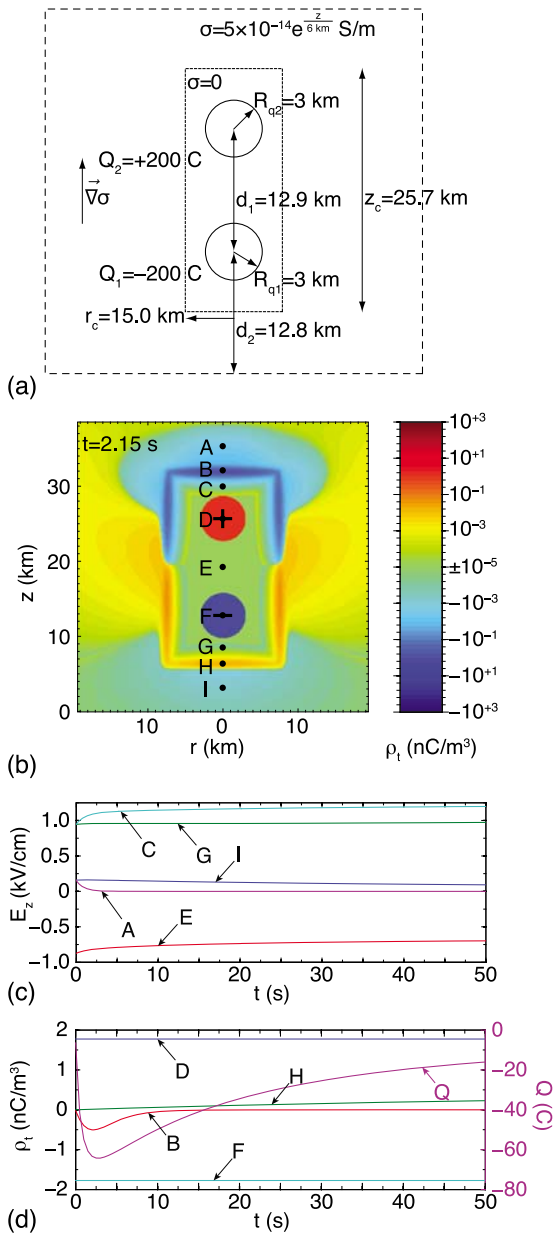


Figure 2. Formation of the screening charge at the boundary of a cylindrically symmetric thundercloud with reduced conductivity. (a) Geometry of the illustrative example. (b) Cross-sectional view of the charge density distribution at $t \sim 2.15$ s. The screening charge develops much faster on the upper boundary of the cylinder than on the lower one because of the exponential increase of conductivity with altitude z . Points A–I indicate the locations where the time evolution of the (c) electric field and (d) charge density, respectively, are shown. The total charge in the simulation domain Q is represented using a solid purple line with corresponding scale shown on the right vertical axis. (See Animations S2a and S2b for the animated version of Figure 2b.)

charge after a few seconds as evidenced by the curve Q versus t shown in Figure 1d. Figure 1d also compares the charge densities at the centers of the two charge regions (points B and D in Figure 1b) with the analytical results

$\rho(z, t) = \rho_0(z) e^{-\frac{\sigma(z)t}{\epsilon_0}}$ for an isolated charge in a uniformly conducting medium, and shows excellent agreement with the numerical results. The example illustrates a simple, plausible way in which storms develop a strong charge imbalance, leading to the occurrence of negative cloud-to-ground discharges (–CG) and to the formation of gigantic jets, as proposed by *Krehbiel et al.* [2008].

[7] The second example, presented in Figure 2 and Animations S2a and S2b, illustrates the effects of embedding the charges in a cloud. Screening charges develop at the cloud boundaries due to conductivity gradients between the clear air outside the storm and the storm’s cloudy interior. The screening charges develop at different rates in the upper and lower part of the storm and enhance the electric field just inside the cloud boundary. These effects can be demonstrated using the same geometry as in Figure 1 with the difference that the dipole is now enclosed in a nonconducting dielectric cylinder. For purposes of illustration, the cylindrical dielectric region has a height (25.7 km) that is significantly greater than the altitude scale of the conductivity variation ($h = 6$ km). Figure 2b shows the charge density distribution after 2.15 s. At this point, screening charges have had enough time to accumulate around the upper boundary of the zero-conductivity region [e.g., *Holzer and Saxon, 1952*] but not around the lower boundary, due to an approximate 70% conductivity difference between these two regions. The evolution of the charge densities at the upper and lower boundary points B and H in Figure 2b is shown in Figure 2d and demonstrates the rate difference. As a result, a dipolar structure is formed between the upper positive charge at location D and the screening charge near point B that increases the electric field at point C between the two charge regions (curve C in Figure 2c and Animation S2b). The local field increase is one of the fundamental effects leading to blue jet initiation discussed by *Krehbiel et al.* [2008]. In both the Figures 1 and 2 examples, the screening process continues until sufficient charge has accumulated to neutralize externally the electric field of the source charge [*Wilson, 1956; Brown et al., 1971*].

[8] The effects discussed above provide additional insight into the initiation of blue and gigantic jets and will be referred to in subsequent sections of this paper. Both blue and gigantic jet discharges are believed to be initiated in a conventional leader form [e.g., *Krehbiel et al., 2008*]. Consequently, we use the 3-D Cartesian model of lightning discharge described by *Riousset et al.* [2007] to model initial development of leaders in specified charge configurations. The same first-principle techniques are used to determine both the lightning charge development and the charge relaxation presented in Figures 1 and 2. These techniques are more fully described in section 2 below.

[9] Classic, normally electrified thunderstorms have a dominant midlevel negative charge region (N) situated between a comparable upper positive charge region (P) above the negative charge, and lesser lower positive charge (LP) below the negative charge [e.g., *Williams, 1989*]. The three charge regions are illustrated in Figures 3a and 3b by blue and red rectangles, respectively. The charges and electric fields build up steadily with time as a result of the storm charging currents until a breakdown threshold is reached. The charging currents are believed to originate

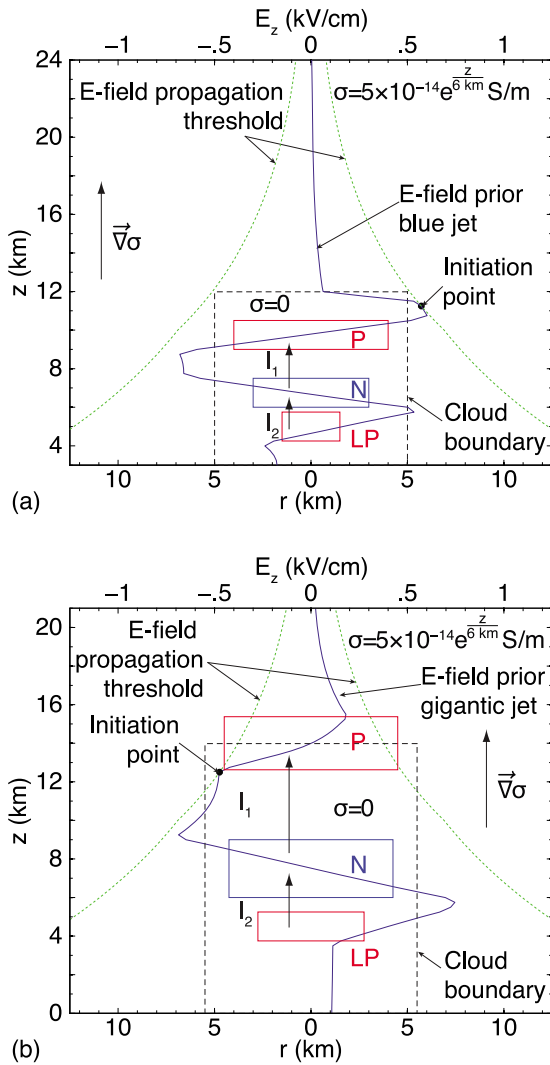


Figure 3. Geometry and conductivity distribution inside and nearby the model cloud employed for the simulation of (a) blue jets and (b) gigantic jets. Dashed green lines represent the electric field threshold E_{th}^{\pm} for lightning initiation. The solid blue lines represent the electric field at $r = 0$ prior to the development of the jets. The solid rectangles marked LP, N, and P depict the altitude and dimensions of the lower positive, central negative, and upper positive thundercloud charge regions, respectively (Tables 1 and 2). The vertical arrows indicate the charging currents I_1 and I_2 .

from convection driven graupel-ice collisions in the presence of supercooled water droplets [e.g., Williams, 1989; Rakov and Uman, 2003, p. 85] and continue to be a topic of active research. Exceeding the breakdown threshold initiates a lightning discharge. Following initiation, bidirectional discharges develop, producing different lightning types depending on where the triggering happens to occur first [Krehbiel et al., 2008]. The discharges suddenly reduce the net charges within the charge regions. The slow and fast time-varying charges in the thunderstorm cause the dynamical formation of induced free charges in the atmosphere and result in the development of so-called *Greifinger and*

Greifingers [1976] boundaries. In an atmosphere with conductivity increasing with altitude a *Greifinger and Greifingers* [1976] boundary separates the regions dominated by displacement current below the boundary and conduction current above the boundary. The location of this boundary depends on the electrodynamics of the thunderstorm in the troposphere. Fast charge rearrangements due to a lightning discharge result in downward moving boundaries while the slow charge buildup due to the storm charging currents leads to the formation of screening charges accumulating at the upper cloud boundary [e.g., Pasko and George, 2002], that can mix with the charge in the upper levels of the cloud. As described on a conceptual level earlier in this section, the screening layer can favor the development of either blue or gigantic jets, depending on the extent to which the screening charge is mixed with the upper storm charge [Krehbiel et al., 2008]. It is believed that after the jets are initiated as regular lightning leader channels, they convert to nonthermal, streamer zone dominated form at higher altitudes [Petrov and Petrova, 1999; Kuo et al., 2009].

2. Model Formulation

[10] To investigate the temporal electrodynamics of thunderclouds leading to jet formation we have developed a 2-D axisymmetric model in which the storm charges are situated inside a cloud of zero electrical conductivity, with the storm as whole being embedded in a conducting atmosphere of increasing conductivity with altitude. The model has radial and vertical domain extents of $L_r = 64.5$ km and $L_z = 72.25$ km, respectively, and is discretized using equidistant grids of 500 m and 250 m in the r and z directions (see Figures 3a and 3b and Table 1).

[11] The thundercloud is assumed to have a classic tripolar charge structure [e.g., Williams, 1989] enclosed in a dielectric cylinder of radius r_c and vertical extent z_c (Table 2) representing the limits of the cloud. The tripole is placed above a perfectly electrically conducting flat ground plane positioned at altitude $z = z_{\text{gnd}}$ (Table 1). The charge regions are modeled as axisymmetric cylindrical disks centered at altitudes z_{LP} , z_N , z_P , and characterized by radii R_{LP} , R_N , R_P , vertical extents d_{LP} , d_N , d_P (Table 2), and net charge contents Q_{LP} , Q_N , Q_P , respectively.

[12] The storm charges are assumed to be generated by charging currents I_1 and I_2 between the N and P regions, and

Table 1. Parameters Used in the Simulations

Name	Symbol	Units	+BJ	-GJ
Ground altitude	z_{gnd}	km	3	0
<i>2-D Axisymmetric Domain</i>				
Dimensions	L_r	km	64.5	64.5
	L_z	km	72.25	72.25
Discretization steps	d_r	m	500	500
	d_z	km	250	250
<i>3-D Cartesian Domain</i>				
Dimensions	L_x	km	18.5	18.5
	L_y	km	18.5	18.5
	L_z	km	21.0	21.0
Discretization steps	d_x	m	500	500
	d_y	m	500	500
	d_z	m	250	250

Table 2. Geometrical and Electrical Parameters of the Model Thundercloud

Name	Symbol	Unit	+BJ	−GJ
<i>Charge Layer Geometry</i>				
Lower positive				
Altitude ^a	z_{LP}	km	2.0	4.5
Radius	R_{LP}	km	1.5	2.75
Depth	d_{LP}	km	1.5	1.5
Central negative				
Altitude ^a	z_N	km	3.75	7.5
Radius	R_N	km	3.0	4.25
Depth	d_N	km	1.5	3.0
Upper positive				
Altitude ^a	z_P	km	6.75	14.0
Radius	R_P	km	4.0	4.5
Depth	d_P	km	1.5	2.75
<i>Cloud Boundaries</i>				
Radius	r_c	km	5	5.5
Height ^a	z_c	km	9	14
Boundary thickness	α	km	0.15	0.75
<i>Charging Currents</i>				
Upper charging current	I_1	A	+1.5	+3.0
Lower charging current	I_2	mA	−90	−250

^aAltitude above ground level.

between the LP and N regions, respectively, as indicated in Figure 3. The source charges are uniformly distributed within each disk and their temporal variation produces time- and space-varying induced free charges ρ_f and electric potentials ϕ both inside and outside the storm. The basic set of equations relating ρ_f and ϕ to the source charge densities ρ_s are

$$\nabla^2 \phi = -\frac{\rho_s + \rho_f}{\epsilon_0} \quad (1)$$

$$\frac{\partial \rho_f}{\partial t} - \nabla \sigma \cdot \nabla \phi = -\sigma \frac{\rho_s + \rho_f}{\epsilon_0} \quad (2)$$

where σ is the atmospheric conductivity. The total charge density is $\rho_t = \rho_s + \rho_f$. The above equations express Gauss's law and conservation of charge, in which the conduction current \vec{J} is assumed to be ohmic and replaced by $\vec{J} = \sigma \vec{E} = -\sigma \nabla \phi$ in (2).

[13] The conductivity σ at any location (r, z) in the simulation domain is expressed by

$$\sigma(r, z) = \underbrace{\sigma_0 e^{-\frac{z+z_{\text{gnd}}}{h}}}_{(I)} \underbrace{\left(1 - \frac{1 - \tanh\left(\frac{r-r_c}{\alpha}\right)}{2} \times \frac{1 - \tanh\left(\frac{z-z_c}{\alpha}\right)}{2} \right)}_{(II)} \quad (3)$$

where the parameter α determines the thickness of the conductivity transition region between the cloud interior and the surrounding clear air. The conductivity outside the cloud increases exponentially with altitude z (term (I) in (3)) with an altitude scaling factor $h = 6$ km and a conductivity at sea level $\sigma_0 = 5 \times 10^{-14}$ S/m [e.g., Pasko et al., 1997, and references therein]. Inside the cloud the conductivity is reduced to zero (term (II) in (3)), with a smooth transition

at the boundary of width $\sim 2\alpha$. Two values of α are used in the simulations, 0.15 and 0.75 km (Table 2), so that the transition region typically contains several (3 to 7) grid points.

[14] Few conductivity measurements have been made inside electrified clouds [MacGorman and Rust, 1998, p. 171 and references therein]. However, because atmospheric ions quickly attach to cloud particles, clouds have a low electrical conductivity [e.g., MacGorman and Rust, 1998, pp. 170–172; Rakov and Uman, 2003, p. 91; Rycroft et al., 2007]. Tests of the sensitivity of the simulation results for both gigantic jets and blue jets to the assumed cloud conductivity (zero and 10% of clear air values; see discussion in the works of MacGorman and Rust [1998, p. 172]) have shown that the results differ only by a slight increase in the charging current required to produce the same charge magnitudes.

[15] The degree to which the screening charge is mixed with the interior, upper positive storm charge is an important factor in the production of blue and gigantic jets. The study by Krehbiel et al. [2008] indicated that blue jets occur most favorably in the absence of mixing, whereas gigantic jets are favored by strong mixing. The two scenarios are currently simulated in the model by having the upper boundary screening charge region overlap or not overlap the upper positive storm charge (Table 2 and Figure 3).

[16] With σ given by (3), we can solve the system (1)–(2) for the two unknowns ϕ and ρ_f . Poisson's equation (1) is solved using a red-black parallel Successive Overrelaxation Method (SOR) [Niethammer, 1989; Zhang et al., 2006], while the continuity equation is solved using a parallel version of the classic Lax scheme [e.g., Potter, 1973, pp. 57 and 67].

[17] The charging currents are chosen to reproduce typical intracloud (IC) and cloud-to-ground (CG) lightning rates in storms believed to produce the two types of jets. Blue jets (BJs) have been observed in electrically active continental storms that produce significant negative cloud-to-ground lightning (−CG) [e.g., Lyons et al., 2003]. On the other hand, gigantic jets (GJs), because they also discharge the N charge region, are predicted to be suppressed by −CG lightning [Krehbiel et al., 2008]. The video recording of a gigantic jet observed from Puerto Rico by Pasko et al. [2002] showed the occurrence of several IC lightning discharges in a rapid succession prior to the jet initiation, implying an active main charging current I_1 . The Puerto Rico event occurred on 14 September 2001 approximately 200 km northwest of Arecibo observatory above a tropical oceanic thunderstorm [Pasko et al., 2002]. Such systems typically produce little cloud-to-ground lightning [e.g., MacGorman and Rust, 1998, pp. 188 and 297] suggesting a relatively small I_2 compared to I_1 . It should be emphasized that the choice of specific values for the charging currents in the simulations does not alter the overall physical interpretation of the electrodynamics of jet-producing storms discussed here.

[18] To model the bulk effect of lightning discharges on the thundercloud electrodynamics, three types of discharges are accounted for: (1) cloud-to-ground discharges (CG), which reduce the net charge content of the LP and N regions by 50% each, (2) intracloud discharges (IC), which cause a reduction of $\min(|Q_N|, |Q_P|)/2$ of the net charge in the N and P layers, and (3) blue jet discharges (BJ), which are assumed to produce a 50% reduction in the screening

charge Q_{SC} and upper positive charge Q_P . These are the parameterizations used in the studies by *Krehbiel et al.* [2004, 2008]. For the GJ simulations, where strong mixing is simulated by overlapping the screening charge with the upper positive charge, IC discharges are assumed to discharge the N and P layers by $\min(|Q_N|, |Q_P + Q_{mix}|)/2$, where Q_{mix} represents the amount of free induced screening charge (corresponding to ρ_f in (1)–(2)) that is present within the confines of the upper positive charge region. In addition, a fourth type of lightning discharge, the gigantic jet discharge, is introduced and assumed to reduce Q_N , Q_P and Q_{SC} each by a factor two, as detailed later in this section.

[19] A discharge is assumed to occur when the electric field exceeds a predefined electric field threshold for initiation and propagation of positive and negative leaders, $E_{th}^{\pm} = 2.16 \times N(z + z_{gnd})/N_0$ kV/cm, where $N(z)$ and N_0 are the neutral densities at altitude z and at sea level, respectively [e.g., *Marshall et al.*, 1995; *Riousset et al.*, 2007, and references therein]. Discrimination between the different types of discharges is based on their initiation altitudes. Breakdown that results from the electric field threshold being exceeded between the LP and N charge regions leads to a negative cloud-to-ground discharge (–CG) in the model that removes 50% of the charge content of the N and LP layers, causing net negative charge to be removed from the cloud (or, equivalently, positive charge to be added). Initiation that occurs between the N and P charge regions generates either an IC or GJ discharge depending on the dynamic charge imbalances in the cloud and the geometrical structure of the charge regions. Finally, if the initial breakdown occurs above the P layer, the model leads to the development of a blue jet event.

[20] A particularly important aspect of the investigations has been to determine when an IC discharge continues on out of the cloud to become a GJ, in which case it behaves like a CG discharge and removes net negative charge from the cloud (–GJ), or if the discharge remains confined within the cloud and produces equal and opposite charge changes and zero net change to the overall storm charge. This determination is made on an *a posteriori* basis by using the fractal discharge model to simulate successive IC discharges until events are found that escape the cloud. From such simulations, an approximate empirical criterion has been developed and used in stand-alone simulations employing only the 2-D electrodynamic model. Whether an IC becomes a GJ depends largely on the relative magnitude of the negative Q_N charge and the mixing-depleted upper positive charge ($Q_P + Q_{mix}$). The fractal simulations indicate that GJs occur when the charge ratio $|Q_P + Q_{mix}|/|Q_N| \lesssim 0.50$. This compares to the nominal criterion assumed for CGs which is that $|Q_{LP}|/|Q_N| < 1$, and a similar criterion for BJs. We emphasize that GJs have a more stringent criterion because the discharge has to propagate through two charge regions rather than one, with the unmixed screening charge being of negative polarity and therefore being repulsive to the escape. Finally, when a GJ is determined or estimated to have occurred, the discharge is assumed in the electrodynamic model to reduce each of the three affected charges (Q_N , Q_P , and Q_{SC}) by half of their original values.

[21] The specific values of the fractional reduction of net electric charge in the charge layers following a discharge are

based on both observational and modeling results and produce discharges with charge transfers that agree well with the estimates available in the referred literature. ICs transfer a few tens of Coulombs between the N and P regions [e.g., *Krehbiel*, 1981; *Krehbiel et al.*, 1984a, 1984b; *Helsdon et al.*, 1992; *Shao and Krehbiel*, 1996; *Rakov and Uman*, 2003, p. 325], while CGs lower similar amounts of charge to the ground in agreement with values reported by *Rakov and Uman* [2003, p. 146]. The model GJ presented in section 3 removed ~ 26 C net negative charge from the storm, consistent with estimates by *Su et al.* [2003]. The fractal model employed in this study has been shown to reproduce well the aforementioned charge transfers [*Riousset et al.*, 2006b, 2007] (see section 3). When reported to the typical net charge content of the thundercloud charge regions [e.g., *Uman*, 2001, p. 60; *Rakov and Uman*, 2003, p. 79], the so-obtained estimates of the fractional charge reduction following a discharge are in a reasonable agreement with the values employed by the thundercloud dynamics model.

[22] During model calculations, the side and top boundaries of the simulation domain are maintained at ground potential (Dirichlet boundary conditions). This hypothesis is fully justified for the ground and ionospheric boundaries [e.g., *Pasko et al.*, 1997] and introduces an error $< 10\%$ on the side boundary, decreasing as one approaches the center of the simulation domain at $r = 0$, i.e., in the region of primary interest. The choice of boundary conditions as well as the choice of a 2-D axisymmetric model is related to the need for a large simulation domain and a very fine time resolution ($0.4 \text{ ms} < \varepsilon_0/\sigma_{max}$, where σ_{max} is the maximum conductivity in the simulation domain), involving a computational time that currently does not allow 3-D modeling.

[23] At the moment of jet initiation, a “still picture” of the charge configuration is taken and converted to 3-D Cartesian coordinates to be used for simulation of the leader trees using the fractal model. The lightning simulation employs the stochastic model described by *Riousset et al.* [2007] and *Krehbiel et al.* [2008] in a reduced size domain enclosing the cloud and its nearest surroundings (see Tables 1 and 2). The use of a simulation domain with reduced size requires Dirichlet open boundary conditions. The open boundary conditions employed in the present work follow procedures described by *Riousset et al.* [2007].

3. Results

[24] In this section we present results from simulation runs leading to blue and gigantic jet events. The examples illustrate the limiting cases of no mixing between the screening and upper positive charges, and nearly complete mixing. These cases give rise to BJs and GJs relatively early and repeatedly in the simulations. In actual storms the mixing is somewhere between the two limits. In addition, potential GJs appear to be converted to bolt from the blue (BFB) discharges, which are relatively common in normally electrified storms [*Thomas et al.*, 2002; *Krehbiel et al.*, 2008].

[25] Figure 3 shows the charge geometry and electric field profiles for two different storms at the time of initiation of a blue jet (Figure 3a) and a gigantic jet (Figure 3b). For clarity of presentation Figures 3a and 3b are focused on the cloud and show only a small part of the 2-D simulation

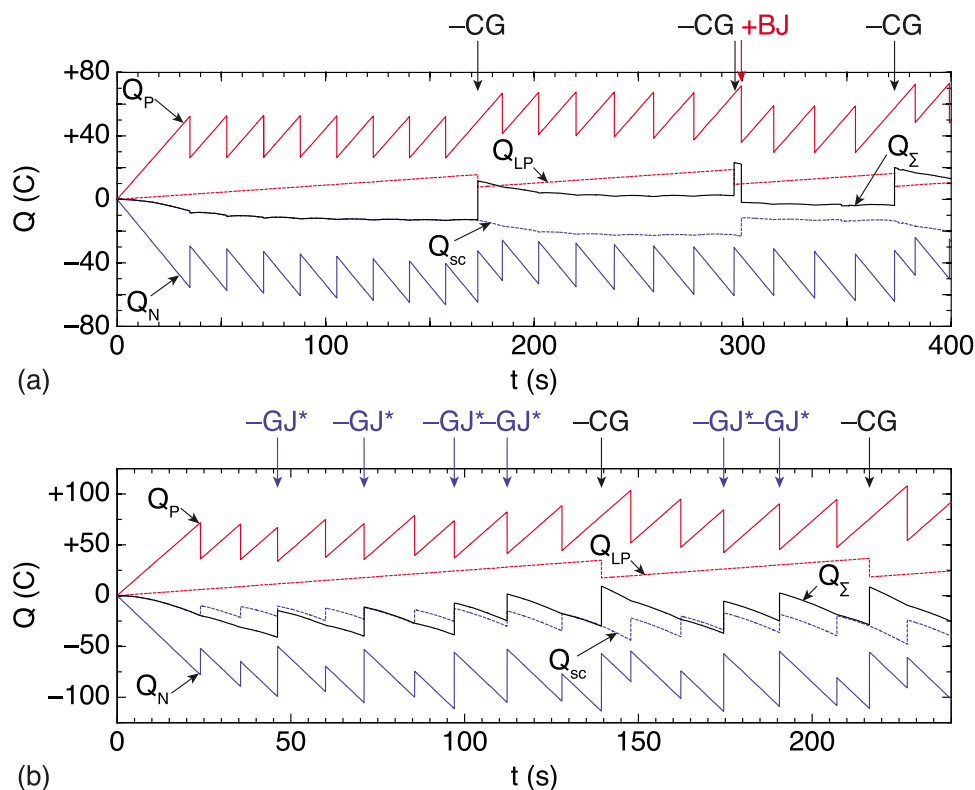


Figure 4. Model-calculated temporal variations of the storm charges leading to initiation of (a) a blue jet discharge between the upper positive layer and the screening charge layer at $t = 299.4$ s and (b) gigantic jet discharges between the central negative layer and upper positive charge layer reduced by the screening charge. The first GJ occurs at $t \sim 46$ s. Sudden vertical jumps in the curves correspond to occurrence of IC discharges unless marked otherwise. Asterisks indicate that the GJs could instead be bolt from the blue discharges.

domain. In Figures 2a and 3b, the vertical arrows indicate the charging currents I_1 and I_2 . The dashed green lines represent the lightning initiation and propagation threshold E_{th}^\pm while the solid blue lines show the electric field at the time of initiation of the jets. The modeled storm of Figure 3a had charging currents of $[I_1, I_2] = [+1.5, -0.09]$ A and a charge structure in which the upper positive charge was separated from the upper cloud boundary and screening charge, so that no mixing occurred between the two. At ~ 300 s into the simulation the initiation threshold was crossed at $z = 11.25$ km, in the enhanced electric field region between the P layer and screening charge and allowing for the development of an upward blue jet (Figures 4a and 5 and Animation S3).

[26] The storm of Figure 3b had a greater vertical extent and an upper cloud boundary centered within the P layer to simulate mixing with the screening charge. The charging currents were also larger, at $[+3.0, -0.25]$ A. The presence of the screening charge within the P layer resulted in the net P charge becoming depleted with time relative to the N charge (Figure 4b and Animation S4). The depletion was such that, ~ 46 s into the simulation, an IC discharge initiated at the base of the P region escaped the cloud as a gigantic jet (Figure 6).

[27] Figure 4a shows the temporal evolution of the blue jet-producing storm of Figure 3a. The storm begins with a

series of eight intracloud discharges between the N and P regions, seen as sudden changes in Q_N and Q_P (solid blue and red traces, respectively). During this time the lower positive charge Q_{LP} (dotted red trace) increased to the point where a -CG discharge was initiated (at ~ 172 s) that changes the overall storm charge Q_Σ (the sum of the four charges Q_{LP} , Q_N , Q_P , and Q_{SC}) from a net negative to net positive value (black trace). The IC/CG sequence is repeated over the next ~ 2 min, after which point a positive blue jet (+BJ) was initiated (Figure 3a). The BJ occurred ~ 4 s after the second -CG and was initiated by virtue of the -CG effectively adding positive charge to the storm, which suddenly increased the electric field in the storm's upper levels [Krehbiel *et al.*, 2008, Figure 1b]. The additional 4 s of charging following the charge-imbalancing -CG caused the BJ breakdown to be initiated before the next IC discharge, which were occurring at ~ 20 s intervals. The BJ caused net positive charge to be removed from the storm, bringing the overall storm charge back close to neutrality. The BJ also discharged part of the negative screening charge Q_{SC} (dotted blue line). We note that the accumulation of screening charge Q_{SC} above the cloud top facilitated the initiation of the BJ. As a consequence of the screening charge being reduced by the BJ, the next CG flash in the sequence did not initiate a BJ. The screening charge did not start to rebuild until after the third -CG caused the storm to

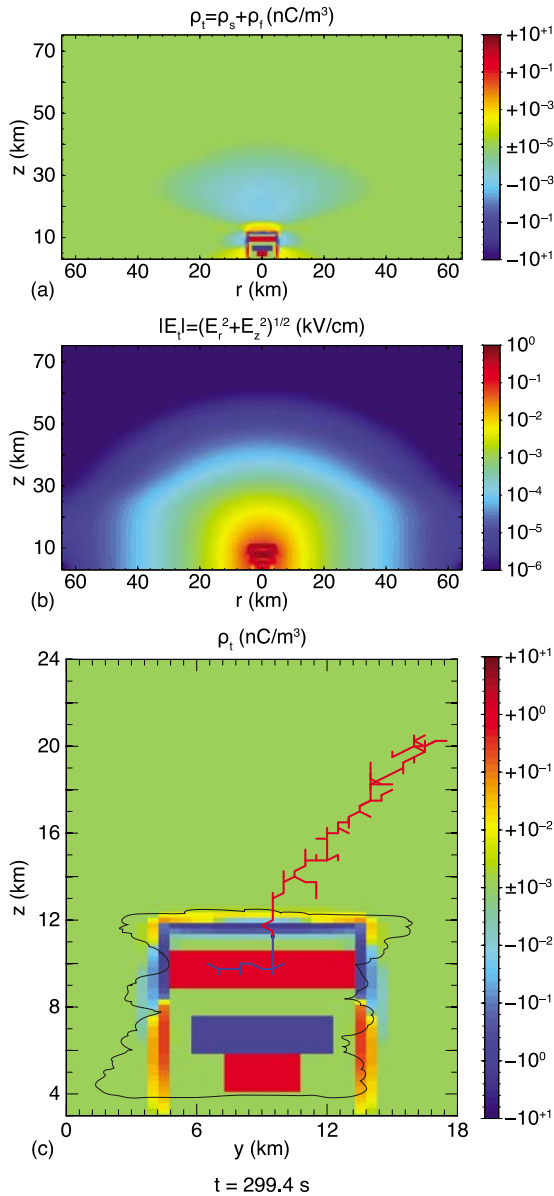


Figure 5. (a) Total charge density and (b) electric field magnitude at the moment of the blue jet initiation $t \sim 299.4$ s (see Figure 4a). At this instant the electric field exceeds the lightning initiation threshold near the cloud upper boundary leading to an upward positive discharge (marked as +BJ in Figure 4a). (c) Modeling of the jet discharge using the 3-D fractal model, with charge densities as background. (See Animation S3 for the animated version of Figures 5a and 5b.)

develop a net positive charge again. Similar results have been obtained using the 1-D model introduced by *Krehbiel et al.* [2004, 2008, supplementary information].

[28] Figure 5a shows the total charge density ρ_t over the entire 2-D simulation domain at the instant of initiation of the blue jet, while Figure 5b shows the magnitude of the electric field at the same instant of time. The zoomed in view of Figure 5c shows how the induced free charges of Figure 5a largely consist of screening charges accumulated at the cloud boundary. Because of being spatially distributed,

the negative component of the screening charge Q_{SC} of Figure 4a is calculated in the model as: $Q_{SC} = \int \int \int_V \rho_f(\vec{r}) dV$, where for simplicity the integration volume V consists of the entire half-space above the lowest altitude z_{bottom} of the upper positive charge region. The integral is dominated by the screening charges on the top and lateral upper cloud boundaries.

[29] Figure 5c also shows a plane projection of the three-dimensionally modeled jet developing under the conditions given by the two-dimensional charge relaxation model. The initiation occurred at $z = 11.25$ km and the discharge developed bidirectionally from that point on, propagating through the screening charge at the top of the cloud, and further developing toward the ionosphere. The simulation

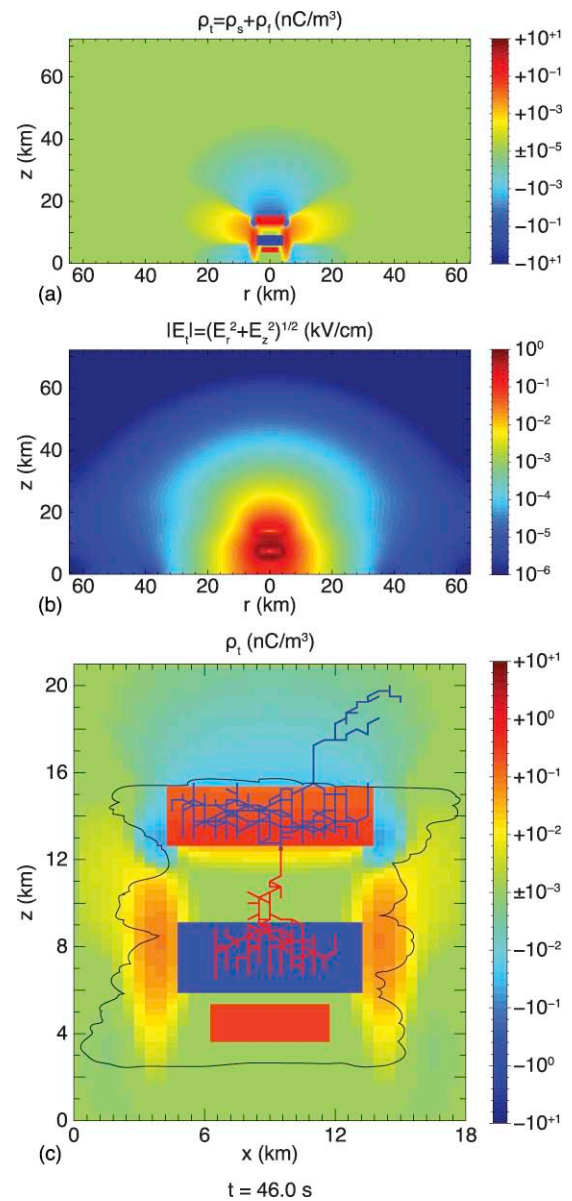


Figure 6. Same as Figure 5, except for the GJ discharge at $t \sim 46$ s in Figure 4b initiated between the central negative and screening depleted upper positive charge regions. (See Animation S4 for the animated version of Figures 6a and 6b.)

was stopped when the discharge exited the simulation domain (through the $y = 0$ km boundary in the present situation, topping at ~ 21 km). Although not modeled in the present work, it is expected [e.g., *Petrov and Petrova*, 1999; *Pasko and George*, 2002; *Krehbiel et al.*, 2008] that the streamer corona of the thermalized leader section of the jet would expand up to higher altitudes, consistent with published observations of blue jets [e.g., *Wescott et al.*, 1995; *Sentman and Wescott*, 1995; *Boeck et al.*, 1995; *Wescott et al.*, 2001].

[30] Figures 4b and 6 present analogous results for the GJ-producing storm of Figure 3b. The larger values of the charging currents ($I_1 = 3.0$ A versus 1.5 A; $I_2 = -0.25$ A versus -90 mA) caused the IC initiation intervals to be shorter (every ~ 13 s) and the first $-CG$ to be initiated after ~ 140 s (Figure 4b). In addition, the higher altitude of the storm causes the screening charge to form relatively rapidly and the storm to accumulate a substantial net negative charge (-40 C) forty seconds into the simulation. By this time, the strong mixing of the screening charge produced an approximate 2:1 charge imbalance between the N and P charge regions, giving rise to a GJ ~ 46 s into the simulation, as the third discharge of the storm. The net effect of the GJ was to release ~ 26 C of negative charge from the storm, similar to a $-CG$ but upward in the atmosphere rather than downward to ground. Under the assumptions (1) that GJs remove only half of the N charge and (2) continued strong mixing, the 3-D discharge model predicts about every other IC to produce an upward $-GJ$. The first $-CG$ briefly interrupted the GJ sequence by providing an alternate way of releasing the accumulated negative charge.

[31] The numerous occurrences of GJs in the simulation suggest that many discharges initiated in the midlevels of a thundercloud are able to escape. Such behavior has been observed in New Mexico thunderstorms, as they commonly develop bolt from the blue (BFB) dominated regimes [*Thomas et al.*, 2002]. Under these circumstances, BFBs become the main discharge process for releasing excess negative charge. The 2-D axisymmetric geometry of the relaxation model does not permit the development of asymmetric, locally enhanced lateral screening charge leading to the development of BFBs [e.g., *Krehbiel et al.*, 2008, Figures 3 and 4e]. Instead, midlevel-initiated escaping discharges develop into gigantic jets. Therefore the repeated occurrence of GJs in Figure 4b is to be expected, and should be compared to a BFB-dominated regime in light of the above argument.

[32] Figure 6a shows the total charge density ρ_t over the entire 2-D simulation domain at the instant of initiation of the gigantic jet, while Figure 6b shows the magnitude of the electric field at the same instant of time. The focused view of Figure 5c shows how the induced free charges of Figure 5a are mixed with and largely contribute to the depletion of the P layer. In this case, the portion Q_{SC} of the free induced charges mixed with the upper positive layer is calculated as $Q_{SC} = Q_{mix} = \iiint_{V_p} \rho_f(\vec{r}) dV$, where the volume of integration V_p is restricted to the volume occupied by the P region itself. Thus, Q_{SC} represents the charge content of the additional layer formed by accumulation of screening charge at the cloud top for the blue jet case, and the amount of screening charge Q_{mix} mixed with Q_p for the gigantic jet case.

[33] Figure 6c shows a plane projection of the three-dimensional model of the first gigantic jet discharge at ~ 46 s. The discharge was initiated at $z = 12.5$ km and developed bidirectionally within and through the N and P layers, respectively. The discharge escaped upward and, as in the blue jet case, the simulation was stopped as the jet reached a boundary of the simulation domain (in this case, the side boundary at $y = 0$ km). As expected for blue jets but not modeled here, the streamer corona of the leader part of gigantic jets is expected to propagate upward toward the ionosphere, consistent with published observations of gigantic jets [e.g., *Pasko et al.*, 2002; *Su et al.*, 2003; *Kuo et al.*, 2009].

4. Discussion

[34] In this section we provide a physical interpretation of the results presented above. In the simulations of blue and gigantic jets, the driving source of all electrical discharges are the charging currents I_1 and I_2 . *Krider and Musser* [1982], *Williams* [1989], and *MacGorman and Rust* [1998, pp. 53–54] reported precipitation currents at the cloud base and at ground from $2\text{--}3$ nA/m² up to 12 nA/m² or more. From the observationally inferred cross section of modeled thunderclouds ($\pi R_{LP}^2 \sim 7.0$ and 25 km² for simulation geometries of Figures 3a and 3b, respectively), the above current densities correspond to a lower-altitude charging current I_2 ranging from ~ 15 mA up to 300 mA. The values of I_2 used in the simulations (90 and 250 mA) and given in Table 2 are therefore in good agreement with observational data. Simulations employing the assumed values of I_2 also give CG flashing rates that are well within the range of observed values.

[35] Few if any direct measurements are available for the main charging current I_1 , but the current can be estimated from IC lightning rates in the storm. Observational data and electrodynamic simulations show that IC discharges transfer up to $20\text{--}40$ C per flash [*Uman*, 1969, pp. 96–101; *Krehbiel*, 1981, p. 143, Tables 8 and 16, and Figure 3.2.31; *Uman*, 1987, pp. 235–237; *Rakov and Uman*, 2003, p. 325]. A modest IC flashing rate of one per 20 s (3 min⁻¹) would therefore require a charging current $I_1 = 1\text{--}2$ A; higher flash rates such as are common in large storms (possibly with decreased charge transfer per flash) would require correspondingly larger charging currents. The values of I_1 used in the simulations (1.5 and 3.0 A) are consistent with such flashing rates.

[36] The model-assumed storm charge densities are on the order of a few nC/m³ (i.e., a few C/km³), and are consistent with in situ balloon measurements (e.g., $2\text{--}6.7$ nC/m³ in the work of *Marshall and Stolzenburg* [1998]). The resulting electric field profiles and magnitudes, $\lesssim 10^5$ V/m (or 1 kV/cm), reasonably match those observed in thunderclouds [*Marshall et al.*, 1995, Figure 3; *Marshall and Stolzenburg*, 2001, Figure 2]. The modeled results constitute slight underestimates of the actual field strengths because the assumed threshold values E_{th}^{\pm} are breakeven values and do not attempt to incorporate an enhancement factor for initiating breakdown, which is not well known.

[37] The conductivity of the moist air within a cloud is decreased due to ion attachment to hydrometeors [e.g., *Brown et al.*, 1971; *Pruppacher and Klett*, 1997, p. 798;

Rakov and Uman, 2003, p. 91] compared to that of the surrounding dry clear air. This results in a conductivity gradient at the cloud boundary (equation (3)) that causes a screening charge to form at the boundary [e.g., MacGorman and Rust, 1998, p. 71]. The location and thickness of the transition from higher to lower conductivity depends on factors like overturning [e.g., Holton, 2004, p. 377] and storm maturity (a description of the thunderstorm evolution can be found in the work of Wallace and Hobbs [1973, p. 351]).

[38] Weak mixing between the upper level screening charge and the cloud interior, due for example to weak overturning, causes a well-defined screening charge to accumulate around the upper cloud boundaries, as seen in Figures 2b and 5c and Animations S1 and S3. The screening charge is of negative polarity and locally enhances the electric field above the upper positive charge layer (Figure 2c). This ultimately results in breakdown occurring in the uppermost part of the cloud that escapes the storm upward and becomes a blue jet. For the simulated storm of Figure 3a, no mixing takes place between the screening and upper positive charges and breakdown occurs quickly in the storm, at ~ 11 km altitude ~ 300 s into the simulation. The jet was triggered ~ 4 s after a $-CG$ discharge that transferred an estimated 20.9 C of negative charge to ground, leaving the storm with an overall net positive charge. The $-CG$ suddenly increased the electric field in the upper storm levels and enabled the next breakdown event to occur above the positive charge region (giving rise to the jet) rather than below the positive charge region (which would have resulted in another IC).

[39] At the time of the jet initiation the lower positive, midlevel negative, upper positive, and cloud top screening charges were $Q_{LP} = +9.7$ C, $Q_N = -35.8$ C, $Q_P = +71.5$ C and $Q_{SC} = -23.3$ C, respectively, corresponding to a net positive charge $Q_\Sigma = +22.1$ C. That the breakdown would result in an upward-escaping discharge is expected from Q_P being more than three times larger than Q_{SC} , and this is confirmed by the three-dimensional fractal modeling. Continued upward propagation is supported by the unconstrained potential profile above the cloud top [Krehbiel et al., 2008, Figure 1f] and by the quasi-exponential decrease of the breakdown threshold with increasing altitude (Figure 3).

[40] It should be noted that BJ breakdown can also occur without the storm having a net positive charge [Krehbiel et al., 2008], as confirmed by other simulations of this study. While a positive charge imbalance helps, the most important factor is that an unmixed screening charge be present, without which the electric field strengths required to trigger breakdown are not reached. This is basically the same reason why lower positive charge is necessary for $-CG$ discharges to be initiated. That BJs occur infrequently in storms, as suggested by the limited number of observations reported to date [e.g., Wescott et al., 1995; Sentman and Wescott, 1995; Boeck et al., 1995; Wescott et al., 2001; Lyons et al., 2003; Chen et al., 2008b], implies that mixing of the screening and upper positive charges is normally strong, as would be expected in convective storms.

[41] The opposite situation, that of strong mixing, results in the upper positive charge becoming depleted, and produces a substantial imbalance between the P and N charges

that enables gigantic jets to occur. Such a situation is expected to occur at or near overshooting tops, in which strong updrafts can loft charged particles high in the storm favoring mixing with the screening charge leading to the charge structure described in Figure 3b. In effect, the upper positive charge is being relaxed away, as in the Figure 1 example (see also Animation S1). At the time of the initial GJ in Figure 3b and Animation S4 ($t = 46.0$ s), $Q_{SC} = Q_{mix} = -20.4$ C of screening charge had mixed with an upper positive charge $Q_P = +67.2$ C, resulting in $+46.8$ C net charge in the upper positive region. By contrast, $Q_N = -99.3$ C, constituting an approximate 2:1 charge imbalance, and producing the first GJ in the fractal simulations.

[42] In a one-dimensional study of bidirectional breakdown processes, [Mazur and Ruhnke, 1998] observed that the upward negative leader of intracloud lightning could continue beyond the upper thundercloud boundary, in the manner of a gigantic jet as discussed above. They consequently recognized possible relationship to prior observations of lightning extending from cloud tops to the stratosphere. However, they attributed their modeling results to the simplified one-dimensional representation of the leader channel in their model that did not allow for horizontal branching in passing through the upper positive charge region. The simplified model of Mazur and Ruhnke [1998] assumed a charge imbalance but the authors did not discuss the physical conditions related to the imbalance, nor did they recognize the role of the screening charge in allowing and/or enabling upward discharge.

[43] Gigantic jets are observed most often above tropical oceanic storms [e.g., Pasko et al., 2002; Su et al., 2003; Chen et al., 2008a, 2008b; Kuo et al., 2009], while only one observation of gigantic jet over land has been reported to date [van der Velde et al., 2007]. Tropical oceanic thunderstorms typically top at higher altitudes than their continental counterparts while producing overall less lightning [MacGorman and Rust, 1998, p. 297]. This weaker lightning activity is believed to be related to the production of gigantic jets as discussed hereafter. Negative cloud-to-ground discharges are the primary means by which normally electrified storms release the excess negative charge resulting from the upper level screening currents. Storms that have a deficit of normally initiated $-CG$ s, coupled with strong mixing, would be favored to return their negative charge upward into the atmosphere by means of negative gigantic jets (or similarly, go indirectly to ground as negative bolts from the blue). In addition, storms that reach relatively high altitudes have their screening charges form relatively rapidly ($\tau_{relax} = 17.2$ s at 14 km altitude) and the upper positive charge to be depleted relatively quickly, further favoring the occurrence of gigantic jets.

[44] Similar to blue jets, the decrease in electric field threshold with altitude supports upward propagation of gigantic jets. We further note that a weak value of I_2 limits the occurrence of negative cloud-to-ground discharges, depriving the thunderstorm of its primary mechanism for eliminating the accumulating negative charge. Figure 4b shows intracloud activity prior to the occurrence of the jet, consistent with the observations of optical flashes recorded by Pasko et al. [2002] (supplementary information, available at <http://pasko.ee.psu.edu/Nature/>) prior to the 14 September

2001 gigantic jet event and more recently by the ISUAL instrument [Kuo *et al.*, 2009].

[45] To illustrate GJ initiation in the model, the screening charge has been allowed to form in the region of the upper positive charge (Table 2), leaving little screening charge that is not mixed with the upper positive charge. Depending on the degree of convective overturning, actual storms will have a partially unmixed negative screening charge above the positive that will serve to impede upward escape. In this case, lightning mapping observations indicate that the discharge escapes sideways out of the cloud to ground as a negative bolt from the blue discharge [e.g., Rison *et al.*, 1999; Thomas *et al.*, 2001]. Positive lateral screening charge [e.g., Krehbiel *et al.*, 2008] (or, possibly, upper positive charge caught in a lateral downdraft) then turns the discharge to ground. Although the screening charge only partially overlaps the upper positive charge, in the presented model only a small fraction of the screening charge is not mixed with the upper positive region leading to relatively easy occurrence of GJs. BFB discharges are commonly observed in normally electrified storms and appear to be enticed downward by positive screening charge that would form laterally around the midlevel negative charge [Krehbiel *et al.*, 2008]. The cylindrically symmetric charge structures of this study do not produce BFB discharges in the fractal simulations, indicating that asymmetrical screening charge accumulations and/or additional positive charge need to be present for BFBs to occur. Tropical oceanic storms may be the primary producer of GJs by virtue of having a tall ‘stovepipe’ structure with strong convective overturning and the upper positive charge having a large vertical separation from the lateral screening charges associated with the midlevel negative charge.

[46] Because of being two-dimensional, the electrodynamic model does not readily allow coupling the results of the 3-D fractal lightning simulations back into the model to further investigate the interactions between lightning and charge structure. Future 3-D versions of the model would enable such studies and also allow the electrodynamic techniques developed in this study to be incorporated into 3-D cloud models. The present 2-D modeling demonstrates that charge structures are produced as an inevitable consequence of the cloud being embedded in a conductive atmosphere, which expected charge accumulations are sufficient to produce blue and gigantic jet-type breakdown. While there may be other ways of creating jet-producing charge configurations, they are not necessary to the development of blue and gigantic jets. Meteorological processes such as high-altitude collisional particle charging, upper level divergence, or wind shear from upstream charge regions may supplement or reduce the role of mixing in the formation of the needed charge configurations. In particular, storm top divergence may play an additional or alternate role in advecting screening charge away from the upper cloud boundary, making it easier for gigantic jets to escape. Conversely, strong horizontal wind shear would primarily affect the screening charge rather than the upper positive charge and therefore would be a detriment to BJs by preventing the screening charge from enhancing the upper level electric field, and to GJs by preventing the screening charge from depleting the upper positive charge region. In addition, advection of the upper positive charge

into the anvil would result in intracloud discharges developing into the anvil instead of going to ground as BFBs or to the lower ionosphere as GJs. In view of these issues, mixing has to be considered as having a strong effect on jet occurrences. The common occurrence of BFB discharges provides clear evidence that the upper positive charge is depleted relative to the midlevel negative charge, which could be a result of mixing processes.

[47] Observations of blue jets [Wescott *et al.*, 1995; Sentman and Wescott, 1995; Boeck *et al.*, 1995; Wescott *et al.*, 2001] and later gigantic jets [Pasko *et al.*, 2002; Su *et al.*, 2003] revealed a fine filamentary structure of these events identified as streamer channels [Pasko and George, 2002, and references therein]. The development of such channels without a lightning leader would require unrealistic amount of charges near the cloud top [Pasko and George, 2002; Rioussset *et al.*, 2006a; Raizer *et al.*, 2007]. The modeling scenarios reported in the present work show how a lightning leader can propagate upward from the cloud, providing a stem above the thundercloud ($z = 20$ km or higher) for development of the streamer corona up to the lower ionosphere, quantitatively demonstrating the idea first expressed by Petrov and Petrova [1999] and further developed in the work of Krehbiel *et al.* [2008].

5. Conclusions

[48] In this paper, we introduced a 2-D axisymmetric model of charge relaxation in the conducting atmosphere. The model was applied in conjunction with Rioussset *et al.*'s [2007] model of lightning to illustrate how blue and gigantic jet discharges are produced above cloud tops. Moreover, the role of the screening charge in the development of each kind of jet discharge is explained through self-consistent modeling. In particular, we demonstrate how the prior occurrence of IC discharges can prevent the development of a blue jet until a cloud-to-ground discharge enhances the excess of positive charge in the cloud by bringing negative charge to ground. The screening charge gradually developing at the cloud top leads to breakdown initiation near the cloud upper boundary, but is insufficient to contain the lightning leader channel within the cloud resulting in occurrence of upward propagating blue jet events. Furthermore, in thunderstorms where convective overturning near the cloud top is sufficiently strong, the screening layer that allowed for blue jet initiation, gets mixed with the storm's upper positive charge region, reducing the net positive charge in this region and causing a substantial charge imbalance between the two main layers of the thundercloud. Quantitative modeling of resulting discharge reveals that the leader channels cannot be contained in the volume enclosed within the cloud boundary and eventually escape upward to form a gigantic jet, consistent with the ideas first expressed by Krehbiel *et al.* [2008].

[49] **Acknowledgments.** The authors thank Ronald J. Thomas for his valuable input on this work and Alfred B. Chen for helpful discussion about ISUAL data. This research was supported by the United States National Science Foundation under grant ATM-0652148 to the Pennsylvania State University and grant ATM-0536950 to the New Mexico Institute of Mining and Technology.

[50] Amitava Bhattacharjee thanks Abram Jacobson and the reviewers for their assistance in evaluating this paper.

References

- Boeck, W. L., O. H. Vaughan, R. J. Blakeslee, B. Vonnegut, M. Brook, and J. McKune (1995), Observations of lightning in the stratosphere, *J. Geophys. Res.*, *100*, 1465–1475.
- Brown, K. A., P. R. Krehbiel, C. B. Moore, and G. N. Sargent (1971), Electrical screening layers around charged clouds, *J. Geophys. Res.*, *76*, 2825–2835.
- Chen, A. B., et al. (2008a), Global distributions and occurrence rates of transient luminous events, *J. Geophys. Res.*, *113*, A08306, doi:10.1029/2008JA013101.
- Chen, A. B., et al. (2008b), Meteorological aspects of elves and jets, *Eos Trans. AGU*, *89*(53), Fall Meet. Suppl., Abstract AE13A-0303.
- Greifinger, C., and P. Greifingers (1976), Transient ULF electric and magnetic fields following a lightning discharge, *J. Geophys. Res.*, *81*, 2237–2247.
- Helsdon, J. H., and R. D. Farley (1987), A numerical modeling study of a Montana thunderstorm: 2. Model results versus observations involving electrical aspects, *J. Geophys. Res.*, *92*, 5661–5675.
- Helsdon, J. H., Jr., G. Wu, and R. D. Farley (1992), An intracloud lightning parameterization scheme for a storm electrification model, *J. Geophys. Res.*, *97*, 5865–5884.
- Holton, J. R. (2004), *An Introduction to Dynamic Meteorology*, Int. Geophys. Ser., vol. 88, 4th ed., 535 pp., Academic, New York.
- Holzer, R., and D. Saxon (1952), Distribution of electrical conduction currents in the vicinity of thunderstorms, *J. Geophys. Res.*, *57*, 207–216.
- Krehbiel, P. R. (1981), An analysis of the electric field change produced by lightning, Ph.D. thesis, Inst. of Sci. and Technol., Univ. of Manchester, Manchester, U. K. (available at <http://hdl.handle.net/10136/92>)
- Krehbiel, P. R., M. Brook, S. Khanna-Gupta, C. Lennon, and R. Lhermitte (1984a), Some results concerning VHF lightning radiation from the real-time LDAR system at KSC, Florida, in *Proceedings of the Seventh International Conference on Atmospheric Electricity*, pp. 388–393, Am. Meteorol. Soc., Albany, N. Y.
- Krehbiel, P. R., R. Tennis, M. Brook, E. W. Holmes, and R. Comes (1984b), A comparative study of the initial sequence of lightning in a small Florida thunderstorm, in *Proceedings of the Seventh International Conference on Atmospheric Electricity*, pp. 279–285, Am. Meteorol. Soc., Albany, N. Y.
- Krehbiel, P., W. Rison, R. Thomas, T. Marshall, M. Stolzenburg, W. Winn, and S. Hunyady (2004), Thunderstorm charge studies using a simple cylindrical charge model, electric field measurements, and lightning mapping observations, *Eos Trans. AGU*, *85*(47), Fall Meet. Suppl., Abstract AE23A-0843.
- Krehbiel, P. R., J. A. Riousset, V. P. Pasko, R. J. Thomas, W. Rison, M. A. Stanley, and H. E. Edens (2008), Upward electrical discharges from thunderstorms, *Nat. Geosci.*, *1*(4), 233–237, doi:10.1038/ngeo162.
- Krider, E. P., and J. A. Musser (1982), Maxwell currents under thunderstorms, *J. Geophys. Res.*, *87*, 11,171–11,176.
- Kuo, C.-L., et al. (2009), Discharge processes, electric field, and electron energy in ISUAL-recorded gigantic jets, *J. Geophys. Res.*, *114*, A04314, doi:10.1029/2008JA013791.
- Liu, N. Y., and V. P. Pasko (2006), Effects of photoionization on similarity properties of streamers at various pressures in air, *J. Phys. D Appl. Phys.*, *39*, 327–334, doi:10.1088/0022-3727/39/2/013.
- Lyons, W. A., T. E. Nelson, R. A. Armstrong, V. P. Pasko, and M. A. Stanley (2003), Upward electrical discharges from thunderstorm tops, *Bull. Am. Meteorol. Soc.*, *84*(4), 445–454, doi:10.1175/BAMS-84-4-445.
- MacGorman, D. R., and W. D. Rust (1998), *The Electrical Nature of Storms*, 432 pp., Oxford Univ. Press, New York.
- Marshall, T. C., and M. Stolzenburg (1998), Estimates of cloud charge densities in thunderstorms, *J. Geophys. Res.*, *103*, 19,769–19,775, doi:10.1029/98JD01674.
- Marshall, T. C., and M. Stolzenburg (2001), Voltages inside and just above thunderstorms, *J. Geophys. Res.*, *106*, 4757–4768.
- Marshall, T. C., M. P. McCarthy, and W. D. Rust (1995), Electric field magnitudes and lightning initiation in thunderstorms, *J. Geophys. Res.*, *100*, 7097–7104, doi:10.1029/95JD00020.
- Mazur, V., and L. H. Ruhnke (1998), Model of electric charges in thunderstorms and associated lightning, *J. Geophys. Res.*, *103*, 23,299–23,308.
- Mishin, E. V., and G. M. Milikh (2008), Blue jets: Upward lightning, *Space Sci. Rev.*, *137*(1–4), 473–488, doi:10.1007/s11214-008-9346-z.
- Niethammer, W. (1989), The SOR method on parallel computers, *Numer. Math.*, *56*, 247–254.
- Pasko, V. P. (2008), Blue jets and gigantic jets: Transient luminous events between thunderstorm tops and the lower ionosphere, *Plasma Phys. Control. Fusion*, *50*(12), 124050, doi:10.1088/0741-3335/50/12/124050.
- Pasko, V. P., and J. J. George (2002), Three-dimensional modeling of blue jets and blue starters, *J. Geophys. Res.*, *107*(A12), 1458, doi:10.1029/2002JA009473.
- Pasko, V. P., U. S. Inan, T. F. Bell, and Y. N. Taranenko (1997), Sprites produced by quasi-electrostatic heating and ionization in the lower ionosphere, *J. Geophys. Res.*, *102*, 4529–4561, doi:10.1029/96JA03528.
- Pasko, V. P., M. A. Stanley, J. D. Matthews, U. S. Inan, and T. G. Wood (2002), Electrical discharge from a thundercloud top to the lower ionosphere, *Nature*, *416*, 152–154, doi:10.1038/416152a.
- Petrov, N. I., and G. N. Petrova (1999), Physical mechanisms for the development of lightning discharges between a thundercloud and the ionosphere, *Tech. Phys.*, *44*, 472–475.
- Potter, D. (1973), *Computational Physics*, 304 pp., John Wiley, New York.
- Pruppacher, H. R., and J. D. Klett (1997), *Microphysics of Clouds and Precipitation*, Atmos. Oceanogr. Sci. Lib. Ser., vol. 18, 2nd ed., 954 pp., Kluwer Acad., Boston, Mass.
- Raizer, Y. P., G. M. Milikh, and M. N. Shneider (2007), Leader–streamers nature of blue jets, *J. Atmos. Sol. Terr. Phys.*, *69*(8), 925–938, doi:10.1016/j.jastp.2007.02.007.
- Rakov, V. A., and M. A. Uman (2003), *Lightning: Physics and Effects*, 850 pp., Cambridge Univ. Press, Cambridge, U. K.
- Riousset, J. A., V. P. Pasko, P. R. Krehbiel, R. J. Thomas, and W. Rison (2006a), Electrical structure of thunderclouds leading to formation of blue jets and gigantic jets, paper presented at 2006 CEDAR Workshop, Abstract COUP-05, Santa Fe, N. M., 22 June.
- Riousset, J. A., V. P. Pasko, P. R. Krehbiel, R. J. Thomas, and W. Rison (2006b), Three-dimensional fractal modeling of intracloud lightning discharge in a New Mexico thunderstorm and comparison with lightning mapping observations, *Eos Trans. AGU*, *87*(52), Fall Meet. Suppl., Abstract AE21A-0996.
- Riousset, J. A., V. P. Pasko, P. R. Krehbiel, R. J. Thomas, and W. Rison (2007), Three-dimensional fractal modeling of intracloud lightning discharge in a New Mexico thunderstorm and comparison with lightning mapping observations, *J. Geophys. Res.*, *112*, D15203, doi:10.1029/2006JD007621.
- Rison, W., R. J. Thomas, P. R. Krehbiel, T. Hamlin, and J. Harlin (1999), A GPS-based three-dimensional lightning mapping system: Initial observations in central New Mexico, *Geophys. Res. Lett.*, *26*, 3573–3576, doi:10.1029/1999GL010856.
- Rycroft, M. J., A. Odzimek, N. F. Arnold, M. Fullekrug, A. Kulak, and T. Neubert (2007), New model simulations of the global atmospheric electric circuit driven by thunderstorms and electrified shower clouds: The roles of lightning and sprites, *J. Atmos. Sol. Terr. Phys.*, *69*(17–18), 2485–2509, doi:10.1016/j.jastp.2007.09.004.
- Sentman, D. D., and E. M. Wescott (1995), Red sprites and blue jets: Thunderstorm-excited optical emissions in the stratosphere, mesosphere, and ionosphere, *Phys. Plasmas*, *2*(6), 2514–2522, doi:10.1063/1.871213.
- Shao, X. M., and P. R. Krehbiel (1996), The spatial and temporal development of intracloud lightning, *J. Geophys. Res.*, *101*, 26,641–26,668.
- Su, H. T., R. R. Hsu, A. B. Chen, Y. C. Wang, W. S. Hsiao, W. C. Lai, L. C. Lee, M. Sato, and H. Fukunishi (2003), Gigantic jets between a thundercloud and the ionosphere, *Nature*, *423*, 974–976, doi:10.1038/nature01759.
- Thomas, R. J., P. R. Krehbiel, W. Rison, T. Hamlin, J. Harlin, and D. Shown (2001), Observations of VHF source powers radiated by lightning, *Geophys. Res. Lett.*, *28*, 143–146.
- Thomas, R. J., S. Behnke, T. Hamlin, J. Harlin, P. Krehbiel, and W. Rison (2002), New Mexico thunderstorms observed by the lightning mapping array: An overview of one season, *Eos Trans. AGU*, *83*(47), Fall Meet. Suppl., Abstract A71B-0097.
- Uman, M. A. (1969), *Lightning*, 264 pp., McGraw-Hill, New York.
- Uman, M. A. (1987), *The Lightning Discharge*, Int. Geophys. Ser., vol. 39, 377 pp., Academic, Orlando, Fla.
- Uman, M. A. (2001), *The Lightning Discharge*, unabridged ed., 377 pp., Dover, Mineola, N. Y.
- van der Velde, O. A., W. A. Lyons, T. E. Nelson, S. A. Cummer, J. Li, and J. Bunnell (2007), Analysis of the first gigantic jet recorded over continental North America, *J. Geophys. Res.*, *112*, D20104, doi:10.1029/2007JD008575.
- Wallace, J. M., and P. V. Hobbs (1973), *Atmospheric Science, An Introductory Survey*, Int. Geophys. Ser., vol. 92, 2nd ed., 504 pp., Academic, New York.
- Wescott, E. M., D. Sentman, D. Osborne, D. Hampton, and M. Heavner (1995), Preliminary results from the Sprites94 aircraft campaign: 2. Blue jets, *Geophys. Res. Lett.*, *22*, 1209–1212.
- Wescott, E. M., D. Sentman, H. C. Stenbaek-Nielsen, P. Huet, M. J. Heavner, and R. Moudry (2001), New evidence for the brightness and ionization of blue jets and blue starters, *J. Geophys. Res.*, *106*, 21,549–21,554, doi:10.1029/2000JA000429.
- Williams, E. R. (1989), The tripolar structure of thunderstorms, *J. Geophys. Res.*, *94*, 13,151–13,167.
- Wilson, C. T. R. (1921), Investigations on lightning discharges and on the electric field of thunderstorms, *Phys. Trans. R. Soc. London A*, *221*, 73–115.

Wilson, C. T. R. (1956), A theory of thundercloud electricity, *Proc. R. Soc. London Ser A*, 236, 297–317.

Zhang, C., H. Lan, Y. Ye, and B. D. Estrade (2006), Parallel SOR iterative algorithms and performance evaluation on a Linux cluster, in *Proceedings of the International Conference on Parallel and Distributed Processing Techniques and Applications, PDPTA 2005*, vol. 1, edited by H. R. Arabnia, pp. 263–269, Comput. Sci. Res. Educ. Appl., Athens, Ga.

J. A. Riouset and V. P. Pasko, CSSL Laboratory, Department of Electrical Engineering, Pennsylvania State University, 211B Electrical Engineering East, University Park, PA 16802, USA. (riouset@psu.edu; vpasko@psu.edu)

W. Rison, Department of Electrical Engineering, New Mexico Institute of Mining and Technology, Socorro, NM 87801, USA. (rison@ee.nmt.edu)

M. A. Stanley, 114 Mesa Verde Rd., Jemez Springs, NM 87025, USA. (sparky@mark-stanley.name)

P. R. Krehbiel, Department of Physics, New Mexico Institute of Mining and Technology, Socorro, NM 87801, USA. (krehbiel@ibis.nmt.edu)